

# Giant enhancement of optical nonlinearity in mixtures of graded particles with dielectric anisotropy

L. Gao<sup>1,2,a</sup>, J.P. Huang<sup>1</sup>, and K.W. Yu<sup>1</sup>

<sup>1</sup> Department of Physics, The Chinese University of Hong Kong, Shatin, New Territories, Hong Kong, P.R. China

<sup>2</sup> Department of Physics, Suzhou University, Suzhou 215 006, P.R. China

Received 16 August 2003

Published online 30 January 2004 – © EDP Sciences, Società Italiana di Fisica, Springer-Verlag 2004

**Abstract.** To investigate the effective linear dielectric constant  $\epsilon_e$  and third-order nonlinear susceptibility  $\chi_e$  of composite media, in which graded inclusions with radial dielectric anisotropy are randomly embedded in a linear isotropic matrix, we develop a nonlinear anisotropic differential effective dipole approximation (NADEDA). Alternatively, based on a first-principles approach, the exact expressions for  $\epsilon_e$  and  $\chi_e$  are also derived for the linear dielectric profiles with small slopes. Then, excellent agreement between the two methods is numerically demonstrated. As an application, we further apply the NADEDA to a nonlinear metal-dielectric composite, in which the metal particles possess spatially varying radial dielectric anisotropy, in an attempt to study the nonlinearity enhancement and the figure of merit of the composite. To this end, it is shown that the presence of gradation in the radial dielectric constant plays a crucial role in enhancing the optical nonlinearity as well as the figure of merit.

**PACS.** 77.22.Ej Polarization and depolarization – 42.65.-k Nonlinear optics – 42.79.Ry Gradient-index (GRIN) devices – 77.84.Lf Composite materials

## 1 Introduction

Graded materials, whose material properties can vary continuously in space, have received much attention [1] as one of the advanced heterogeneous composites in various engineering applications by using the gradients in thermal [2], electric [3] and mechanical properties [4]. In nature, there are also many graded materials, such as liquid crystal droplets [5] and biological cells [6], because of the inhomogeneous compartment inside them. Physically, graded materials are quite different from the homogeneous ones and other conventional composites. Therefore, the composite media consisting of graded particles can be more useful and interesting than those of homogeneous inclusions. Recently, a first-principles approach [7, 8] and a differential effective dipole approximation [9, 10] have been put forward to study the dielectric response of graded materials.

The above original gradation models were built up under the assumption that the graded inclusions exhibit isotropic dielectric response. However, dielectric anisotropy occurs naturally due to the presence of gradation inside the particles. Moreover, there are many inhomogeneous materials with spatial anisotropy, like polycrystal aggregates of a single anisotropic component [11],

liquid crystal droplets [12], and cell membranes containing mobile charges [13]. In these situations, the local dielectric coefficient should be tensorial. Thus, for a better understanding of the dielectric-anisotropy effect, it is necessary to generalize our previous isotropic gradation models [7–10] accordingly.

The problem is further complicated by the fact that, in realistic composites, besides the inhomogeneity and anisotropy, the nonlinearity plays an important role in determining the effective material properties of realistic composite media [14–16]. Actually, the nonlinearity is a common phenomena in realistic graded materials. And the spatial anisotropy effect has not yet been investigated in the traditional theories. In this work, we shall develop a new theory, in an attempt to study the effective linear and nonlinear optical properties of composite media, by taking into account the dielectric anisotropy of the nonlinear graded particles. For the dielectric tensor of these graded inclusions, the components of the tensorial dielectric constant of interest will be assumed to vary along the radius of the particles continuously.

The paper is organized as follows. The next section describes briefly the model and the definition of the effective linear dielectric constant ( $\epsilon_e$ ) and third-order nonlinear susceptibility ( $\chi_e$ ). In Section 3, we develop the nonlinear anisotropic differential effective dipole

<sup>a</sup> e-mail: lgaophys@pub.sz.jsinfo.net

approximation (NADEDA) for estimating  $\epsilon_e$  and  $\chi_e$  of nonlinear composite media of graded inclusions with anisotropic dielectric constant. In Section 4, to show the validity of the NADEDA, based on a first-principles approach, we derive exactly the analytical expressions for composite media with linear dielectric gradation profiles inside the anisotropic inclusions, which is followed by the numerical results in Section 5. The discussion and conclusion will be given in Section 6.

## 2 Model and definition of effective linear dielectric constant and third-order nonlinear susceptibility

Let us consider a dilute composite material, where the identical spherical inclusions having a dielectric constant tensor  $\vec{\epsilon}_1$ , with radius  $a$ , are randomly embedded in a linear isotropic host with (scalar) dielectric constant  $\epsilon_2$ . Inside the anisotropic inclusions, the local constitutive relation between the displacement ( $\mathbf{D}$ ) and the electric field ( $\mathbf{E}$ ) is given by [18]

$$D_i = \sum_j \epsilon_{ij} E_j + \sum_{ijkl} \chi_{ijkl} E_j E_k E_l^*. \quad (1)$$

Here  $D_i$  and  $E_i$  are respectively the  $i$ -th Cartesian components of  $\mathbf{D}$  and  $\mathbf{E}$ . It is worth remarking that  $\epsilon_{ij}$  and  $\chi_{ijkl}$  are the second-rank and fourth-rank Cartesian tensors, respectively. Throughout the paper, our analysis will be limited to the case of weak nonlinearity. In other words, the nonlinear part in equation (1) will be assumed to be small when compared with the linear part.

In what follows, the dielectric tensor for the the anisotropic spherical inclusions is assumed to be diagonal in spherical coordinates, with a value  $\epsilon_{1t}(r)$  in the tangential directions and  $\epsilon_{1r}(r)$  in the radial direction [13,17]. Here, both dielectric gradation profiles  $\epsilon_{1r}(r)$  and  $\epsilon_{1t}(r)$  will be mathematically represented as radial functions [17]. In view of the spherical symmetry, we can express the dielectric constant tensor  $\vec{\epsilon}_1(r)$  of graded particles in the form

$$\vec{\epsilon}_1(r) = \begin{pmatrix} \epsilon_{1r}(r) & 0 & 0 \\ 0 & \epsilon_{1t}(r) & 0 \\ 0 & 0 & \epsilon_{1t}(r) \end{pmatrix}. \quad (2)$$

Note the above form is in spherical coordinates, rather than in Cartesian coordinates. Nevertheless, it can also be represented in Cartesian coordinates by a transformation using appropriate rotation matrices.

As the graded inclusions with dielectric anisotropy are randomly oriented, the whole sample should be macroscopically isotropic. Thus, we can define the effective linear dielectric constant  $\epsilon_e$  and the third-order nonlinear susceptibility  $\chi_e$  of the whole composite as [18,19]

$$\langle \mathbf{D} \rangle = \epsilon_e \mathbf{E}_0 + \chi_e |\mathbf{E}_0|^2 \mathbf{E}_0, \quad (3)$$

where  $\langle \cdot \cdot \cdot \rangle$  stands for the spatial average, and  $\mathbf{E}_0 = E_0 \mathbf{e}_z$  denotes the external applied field along  $z$ -axis. In equation (3), the effective linear dielectric constant  $\epsilon_e$  is given by

$$\begin{aligned} \epsilon_e \mathbf{E}_0 &= \frac{1}{V} \int_V \vec{\epsilon} \cdot \mathbf{E}_{\text{lin}} dV \\ &= f \langle \vec{\epsilon}_1 \cdot \mathbf{E}_{1,\text{lin}} \rangle + (1-f) \epsilon_2 \langle \mathbf{E}_{2,\text{lin}} \rangle, \end{aligned} \quad (4)$$

where  $f$  is the volume fraction of the graded inclusions. Here, the subscript 'lin' denotes the linear local field inside the graded inclusions or the host.

In view of the existence of nonlinearity inside the anisotropic graded particles,  $\chi_e$  is given by [19,20]

$$\begin{aligned} \chi_e |E_0|^2 E_0^2 &= \frac{1}{V} \sum_{ijkl} \int_V \chi_{ijkl} E_{\text{lin},i} E_{\text{lin},j} E_{\text{lin},k} E_{\text{lin},l}^* dV \\ &= f \sum_{ijkl} \langle \chi_{ijkl} E_{\text{lin},i} E_{\text{lin},j} E_{\text{lin},k} E_{\text{lin},l} \rangle. \end{aligned} \quad (5)$$

Here  $E_{\text{lin},i}$  denotes the Cartesian component of the linear local electric field. Then, just as in isotropic composites [19], both  $\epsilon_e$  and  $\chi_e$  in nonlinear composite media with local dielectric anisotropy can be expressed (to the lowest order in the nonlinearity) in terms of the electric field in the related linear medium as well.

In the next section, we will develop an NADEDA (nonlinear anisotropic differential effective dipole approximation), so as to derive the equivalent linear dielectric constant  $\bar{\epsilon}(a)$  and third-order nonlinear susceptibility  $\bar{\chi}(a)$  of the nonlinear graded inclusions. In this connection,  $\epsilon_e$  and  $\chi_e$  of this anisotropic graded composite media can further be derived in the dilute limit.

## 3 Nonlinear anisotropic differential effective dipole approximation

To put forth an NADEDA (nonlinear anisotropic differential effective dipole approximation) for graded particles with dielectric anisotropy, we regard the gradation profiles as a multi-shell construction. In detail, we build up the dielectric profile by adding shells gradually [10]. Let us start with an infinitesimal spherical core with linear dielectric constants  $\epsilon_{1r}(r=0) = \epsilon_{1t}(r=0) = \epsilon(0)$  and nonlinear susceptibility  $\chi_{ijkl}$ , and keep on adding shells with the tangential and radial dielectric constant  $\epsilon_{1r}(r)$  and  $\epsilon_{1t}(r)$ , and the Cartesian fourth-rank tensorial nonlinear susceptibility  $\chi_{ijkl}$  (to show the optical nonlinearity enhancement, we always assume  $\chi_{ijkl}$  to be independent of  $r$ ), at radius  $r$ , until  $r = a$  is reached.

At radius  $r$ , we have an inhomogeneous spherical particle with spatially varying dielectric constant, which are characterized by the gradation profiles  $\epsilon_{1r}(r)$  and  $\epsilon_{1t}(r)$ , and with tensorial nonlinear susceptibility  $\chi_{ijkl}$ . Then, we can regard such an inhomogeneous particle as an effective *homogeneous* one with the equivalent isotropic dielectric properties  $\bar{\epsilon}(r)$  and  $\bar{\chi}(r)$ . Here the *homogeneous* sphere

$$\begin{aligned}\bar{\epsilon}(r+dr) &= \epsilon_{1r}(r) \left\{ 1 + \frac{\bar{\epsilon}(r) [(\delta-1) + (\delta+2)\lambda^{(1+2\delta)/3}] + \epsilon_{1r}(r) [(\delta^2-1) - (\delta+2)\delta\lambda^{(1+2\delta)/3}]}{\bar{\epsilon}(r)(1-\lambda^{(1+2\delta)/3}) + \epsilon_{1r}(r)[\delta+1+\delta\lambda^{(1+2\delta)/3}]} \right\} \\ &= \bar{\epsilon}(r) + \frac{[\delta\epsilon_{1r}(r) - \bar{\epsilon}(r)][(\delta+1)\epsilon_{1r}(r) + \bar{\epsilon}(r)]}{r\epsilon_{1r}(r)} dr.\end{aligned}\quad (10)$$

should induce the same dipole moment as the original inhomogeneous sphere. Then, we add to the *homogeneous* particle a spherical shell of infinitesimal thickness  $dr$ , with linear dielectric constants,  $\epsilon_{1r}(r)$  and  $\epsilon_{1t}(r)$ , and nonlinear susceptibility,  $\chi_{ijkl}$ . In this situation, the coated inclusions are composed of a spherical core with radius  $r$ , linear dielectric constant  $\bar{\epsilon}(r)$  as well as nonlinear susceptibility  $\bar{\chi}(r)$ , and a shell with outermost radius  $r+dr$ , linear dielectric constants  $\epsilon_{1r}(r)$  and  $\epsilon_{1t}(r)$ , as well as nonlinear susceptibility  $\chi_{ijkl}$ .

For the graded particles with dielectric anisotropy describe equation (2), the displacement vector is related to the field,  $\mathbf{D} = \vec{\epsilon}_1(r) \cdot \mathbf{E}$ . In view of  $\mathbf{E} = -\nabla\Phi$ , we have the following electrostatic equation,

$$\nabla \cdot (\vec{\epsilon}_1(r) \cdot \nabla\Phi) = 0. \quad (6)$$

In spherical coordinates, equation (6) can be cast into,

$$\begin{aligned}\frac{1}{r^2} \frac{\partial}{\partial r} \left( r^2 \epsilon_{1r}(r) \frac{\partial\Phi}{\partial r} \right) + \frac{1}{r^2 \sin\theta} \frac{\partial}{\partial\theta} \left( \sin\theta \epsilon_{1t}(r) \frac{\partial\Phi}{\partial\theta} \right) \\ + \frac{1}{r^2 \sin^2\theta} \frac{\partial}{\partial\psi} \left( \epsilon_{1t}(r) \frac{\partial\Phi}{\partial\psi} \right) = 0.\end{aligned}\quad (7)$$

Let's consider the composite where the coated inclusions are randomly embedded in the linear host medium. Under the quasi-static approximation, we can readily obtain the linear electric potentials inside the core, shell and host medium by solving equation (7),

$$\begin{aligned}\phi_c &= -E_0 AR \cos\theta, & R < r, \\ \phi_s &= -E_0 \left( B(r+dr)^{1-\delta} R^\delta - \frac{Cr^{(1+2\delta)}(r+dr)^{1-\delta}}{R^{\delta+1}} \right) \cos\theta, \\ & r < R < r+dr, \\ \phi_h &= -E_0 \left( R - \frac{D(r+dr)^3}{R^2} \right) \cos\theta, & R > r+dr.\end{aligned}\quad (8)$$

Here the four unknown parameters  $A$ ,  $B$ ,  $C$  and  $D$  can be determined by applying the appropriate boundary condi-

tions on the interfaces. As a result, we obtain

$$\begin{aligned}A &= \frac{3(1+2\delta)\epsilon_2\epsilon_{1r}(r)\lambda^{(\delta-1)/3}}{Q}, \\ B &= \frac{3\epsilon_2[\bar{\epsilon}(r) + (1+\delta)\epsilon_{1r}(r)]}{Q}, \\ C &= \frac{3\epsilon_2[\bar{\epsilon}(r) - \delta \cdot \epsilon_{1r}(r)]}{Q}, \\ D &= \frac{[\delta \cdot \epsilon_{1r}(r) - \epsilon_2][\bar{\epsilon}(r) + (1+\delta)\epsilon_{1r}(r)]}{Q} \\ &\quad + \frac{\lambda^{(1+2\delta)/3}[\epsilon_2 + (1+\delta)\epsilon_{1r}(r)][\bar{\epsilon}(r) - \delta \cdot \epsilon_{1r}(r)]}{Q},\end{aligned}$$

with interfacial parameter  $\lambda \equiv [r/(r+dr)]^3$  and  $\delta \equiv -1/2 + \sqrt{1/4 + 2\epsilon_{1t}(r)/\epsilon_{1r}(r)}$ , and

$$\begin{aligned}Q &= [\delta \cdot \epsilon_{1r}(r) + 2\epsilon_2][\bar{\epsilon}(r) + (1+\delta)\epsilon_{1r}(r)] \\ &\quad + \lambda^{(1+2\delta)/3}[(1+\delta)\epsilon_{1r}(r) - 2\epsilon_2][\bar{\epsilon}(r) - \delta \cdot \epsilon_{1r}(r)].\end{aligned}$$

If  $\epsilon_{1t}(r) = \epsilon_{1r}(r)$ , the physical parameter  $\delta = 1$ , and then equation (8) degenerates to the isotropic form.

The effective (overall) linear dielectric constant of the system is determined by the dilute-limit expression [21]

$$\epsilon_e = \epsilon_2 + 3p\epsilon_2 D, \quad (9)$$

where  $p$  is the volume fraction of the graded particles with radius  $r$ . The equivalent dielectric constant  $\bar{\epsilon}(r+dr)$  for the graded particles with radius  $r+dr$  can be self-consistently obtained by the vanishing of the dipole factor  $D$  by replacing  $\epsilon_2$  with  $\bar{\epsilon}(r+dr)$ . Taking the limit  $dr \rightarrow 0$  and keeping to the first order in  $dr$ , we obtain

See equation (10) above

Thus, we have the differential equation for the equivalent dielectric constant  $\bar{\epsilon}(r)$ ,

$$\frac{d\bar{\epsilon}(r)}{dr} = \frac{\delta(\delta+1)[\epsilon_{1r}(r)]^2 - \bar{\epsilon}(r)\epsilon_{1r}(r) - [\bar{\epsilon}(r)]^2}{r\epsilon_{1r}(r)}. \quad (11)$$

Note that equation (11) is just the Tartar formula, which was derived for assemblages of spheres with varying radial and tangential conductivity [22]. If  $\epsilon_{1r}$  is independent of  $r$ , namely  $\epsilon_{1r} = \epsilon_1$ , we have  $\delta = 1$  due to isotropic property at  $r = 0$ , and then equation (11) predicts  $\bar{\epsilon}(r) = \epsilon_1$ , as expected.

Next, we speculate on how to derive the equivalent nonlinear susceptibility  $\bar{\chi}(r)$ . After applying equation (5) to the coated particles with radius  $r + dr$ , we have

$$\bar{\chi}(r + dr) \frac{\langle |E|^2 E^2 \rangle_{R \leq r+dr}}{|E_0|^2 E_0^2} = \lambda \bar{\chi}(r) \frac{\langle |E|^2 E^2 \rangle_{R \leq r}}{|E_0|^2 E_0^2} + (1 - \lambda) \frac{\sum_{ijkl} \langle \chi_{ijkl} E_i E_j E_k E_l^* \rangle_{r < R \leq r+dr}}{|E_0|^2 E_0^2}. \quad (12)$$

As  $dr \rightarrow 0$ , the left-hand side of the above equation admits

$$\begin{aligned} \bar{\chi}(r + dr) \frac{\langle |E|^2 E^2 \rangle_{R \leq r+dr}}{|E_0|^2 E_0^2} &= \\ \bar{\chi}(r + dr) \left| \frac{3\epsilon_2}{\bar{\epsilon}(r + dr) + 2\epsilon_2} \right|^2 \left( \frac{3\epsilon_2}{\bar{\epsilon}(r + dr) + 2\epsilon_2} \right)^2 & \\ = \bar{\chi}(r) |K|^2 K^2 - dr \bar{\chi}(r) |K|^2 K^2 \left[ \frac{3d\bar{\epsilon}(r)/dr}{2\epsilon_2 + \bar{\epsilon}(r)} \right. & \\ \left. + \left( \frac{d\bar{\epsilon}(r)/dr}{2\epsilon_2 + \bar{\epsilon}(r)} \right)^* \right] + |K|^2 K^2 \frac{d\bar{\chi}(r)}{dr} \cdot dr, & \quad (13) \end{aligned}$$

with  $K = (3\epsilon_2)/[\bar{\epsilon}(r) + 2\epsilon_2]$ . The first part of the right-hand side of equation (12) is written as

$$\lambda \frac{\bar{\chi}(r) \langle |E|^2 E^2 \rangle_{R \leq r}}{|E_0|^2 E_0^2} = \bar{\chi}(r) |K|^2 K^2 \left[ 1 + (3y + y^* - 3) \frac{dr}{r} \right], \quad (14)$$

where

$$y = \frac{[(1 + \delta)\epsilon_{1r}(r) - 2\epsilon_2][\bar{\epsilon}(r) - \delta \cdot \epsilon_{1r}(r)]}{\epsilon_{1r}(r)[\bar{\epsilon}(r) + 2\epsilon_2]} - \delta + 1.$$

The term  $U \equiv (\sum_{ijkl} \langle \chi_{ijkl}(r) E_i E_j E_k E_l^* \rangle_{r < R \leq r+dr}) / (|E_0|^2 E_0^2)$  in equation (12) is written as,

$$\begin{aligned} U &= [( \chi_{xxyy} + \chi_{yxxy} + \chi_{xyxy} + \chi_{xyyx} + \chi_{yxyx} + \chi_{yyxx} \\ &+ 3\chi_{xxxx} + 3\chi_{yyyy} ) U_{p1} ( \chi_{xxzz} + \chi_{zzxx} + \chi_{zzxx} \\ &+ \chi_{zyyz} + \chi_{yzyz} + \chi_{yyzz} ) U_{p2} + ( \chi_{zzxx} + \chi_{zzxx} \\ &+ \chi_{zzxx} + \chi_{yzyy} + \chi_{zyzy} + \chi_{zzyy} ) \\ &\times U_{p3} + \chi_{zzzz} U_{p4}] \frac{|K|^2 K^2}{315}, \quad (15) \end{aligned}$$

where

$$\begin{aligned} U_{p1} &= [B_2(\delta - 1) + C_2(2 + \delta)]^3 \cdot [B_2^*(\delta - 1) + C_2^*(2 + \delta)], \\ U_{p2} &= [B_2(\delta - 1) + C_2(2 + \delta)]^2 \cdot [|C_2|^2(5 + 2\delta + 5\delta^2) \\ &+ (C_2 B_2^* + B_2 C_2^*)(-4 + 5\delta + 5\delta^2) \\ &+ |B_2|^2(8 + 8\delta + 5\delta^2)], \\ U_{p3} &= [B_2^*(\delta - 1) + C_2^*(2 + \delta)] \cdot [B_2^3(-8 + 3\delta^2 + 5\delta^3) \\ &+ 3B_2^2 C_2(8 + 2\delta + 6\delta^2 + 5\delta^3) + 3B_2 C_2^2(-7 + 5\delta \\ &+ 9\delta^2 + 5\delta^3) + C_2^3(10 + 9\delta + 12\delta^2 + 5\delta^3)], \\ U_{p4} &= [B_2^* |B_2|^2(128 + 64\delta + 48\delta^2 + 40\delta^3 + 35\delta^4) \\ &+ B_2^2(3C_2 B_2^* + B_2 C_2^*)(-112 - 8\delta + 30\delta^2 + 55\delta^3 \\ &+ 35\delta^4) + 3B_2 C_2(C_2 B_2^* + B_2 C_2^*)(104 + 4\delta + 39\delta^2 \\ &+ 70\delta^3 + 35\delta^4) + C_2^2(C_2 B_2^* + 3B_2 C_2^*)(-94 + 43\delta \\ &+ 75\delta^2 + 85\delta^3 + 35\delta^4) + C_2^2 |C_2|^2(107 + 52\delta \\ &+ 138\delta^2 + 100\delta^3 + 35\delta^4)], \end{aligned}$$

with

$$B_2 = \frac{\bar{\epsilon}(r) + (1 + \delta)\epsilon_{1r}(r)}{(1 + 2\delta)\epsilon_{1r}(r)} \quad \text{and} \quad C_2 = \frac{\bar{\epsilon}(r) - \delta \cdot \epsilon_{1r}(r)}{(1 + 2\delta)\epsilon_{1r}(r)}.$$

Substituting equations (13, 14) and (15) into equation (12), we have a differential equation for the equivalent nonlinear susceptibility  $\bar{\chi}(r)$ , namely,

$$\begin{aligned} \frac{d\bar{\chi}(r)}{dr} &= \bar{\chi}(r) \left[ \frac{3d\bar{\epsilon}(r)/dr}{2\epsilon_2 + \bar{\epsilon}(r)} + \left( \frac{d\bar{\epsilon}(r)/dr}{2\epsilon_2 + \bar{\epsilon}(r)} \right)^* \right] \\ &+ \bar{\chi}(r) \cdot \frac{3y + y^* - 3}{r} + \frac{3}{r} \cdot \frac{U}{|K|^2 K^2}. \quad (16) \end{aligned}$$

From equations (15, 16), it is evident that  $\chi_{ijkl}$  does not contribute to the equivalent nonlinear susceptibility, except for the cases with equal pair indices.

So far, the equivalent  $\bar{\epsilon}(r)$  and  $\bar{\chi}(r)$  of the anisotropic graded spherical particles with radius  $r$  can be calculated, at least numerically, by solving the differential equations (11) and (16), as long as  $\epsilon_{1r}(r)$ ,  $\epsilon_{1t}(r)$  (dielectric-constant gradation profiles) and  $\chi_{ijkl}$  are given. Here we would like to mention that, even though  $\chi_{ijkl}$  is independent of  $r$ , the equivalent  $\bar{\chi}(r)$  should still be dependent on  $r$ . This is because both  $\epsilon_{1r}(r)$  and  $\epsilon_{1t}(r)$  are  $r$ -dependent. Moreover, if  $\chi_{ijkl} = 0$ , equation (12) admits  $\bar{\chi}(r) = 0$ , as expected as well.

To obtain  $\bar{\epsilon}(r = a)$  and  $\bar{\chi}(r = a)$ , we integrate equations (11) and (16) numerically, for given initial conditions  $\bar{\epsilon}(r \rightarrow 0)$  and  $\bar{\chi}(r \rightarrow 0)$ . Once  $\bar{\epsilon}(r = a)$  and  $\bar{\chi}(r = a)$  are calculated, we can take one step forward to work out the

effective linear and nonlinear responses of the whole composite  $\epsilon_e$  and  $\chi_e$  [18],

$$\epsilon_e = \epsilon_2 + 3\epsilon_2 f \frac{\bar{\epsilon}(r=a) - \epsilon_2}{\bar{\epsilon}(r=a) + 2\epsilon_2}, \quad (17)$$

and

$$\chi_e = f \bar{\chi}(r=a) \left| \frac{3\epsilon_2}{\bar{\epsilon}(r=a) + 2\epsilon_2} \right|^2 \left( \frac{3\epsilon_2}{\bar{\epsilon}(r=a) + 2\epsilon_2} \right)^2. \quad (18)$$

#### 4 Exact solution for linear gradation profiles

Based on the first-principles approach, the potentials within the graded inclusions and the host medium can be exactly obtained, when the dielectric gradation profiles are the linear radial functions with small slopes, i.e.,  $\epsilon_{1r}(r) = \epsilon(0) + g(r/a)$  and  $\epsilon_{1t}(r) = \epsilon(0) + h(r/a)$ . Here  $g$  [ $< a\epsilon(0)$ ] and  $h$  are two constants, and  $\epsilon(0)$  denotes the linear dielectric constant at radius  $r = 0$ .

The potentials within the graded spheres and the host medium are respectively given by

$$\begin{aligned} \phi_c(r, \theta) &= -E_0 A_1 \sum_{k=0}^{\infty} C_k \left( \frac{gr}{a\epsilon(0)} \right)^{k+1} \cos\theta, \quad r < a, \\ \phi_m(r, \theta) &= -E_0 r \cos\theta + \frac{D_1}{r^2} E_0 \cos\theta, \quad r > a, \end{aligned} \quad (19)$$

where the coefficients  $A_1$  and  $D_1$  have the following forms

$$\begin{aligned} A_1 &= \frac{3\epsilon_2 a}{(\epsilon(0) + g)v_2 + 2\epsilon_2 v_1} \quad \text{and} \\ D_1 &= \frac{(\epsilon(0) + g)v_2 - \epsilon_2 v_1}{(\epsilon(0) + g)v_2 + 2\epsilon_2 v_1} a^3. \end{aligned}$$

Here  $v_1$  and  $v_2$  are given by

$$\begin{aligned} v_1 &= \sum_{k=0}^{\infty} C_k \left( \frac{g}{\epsilon(0)} \right)^{k+1} \quad \text{and} \\ v_2 &= \sum_{k=0}^{\infty} C_k (k+1) \left( \frac{g}{\epsilon(0)} \right)^{k+1}, \end{aligned}$$

with  $C_k$  satisfying the following recurrent relation,

$$C_{k+1} = -\frac{(k+1)(k+3) - 2h/g}{(k+2)(k+3) - 2} C_k.$$

The local electric field inside the anisotropic graded inclusions can be derived from the relation  $\mathbf{E} = -\nabla\phi$ , and we have

$$\begin{aligned} \mathbf{E}_c &= A_1 E_0 \sum_{k=0}^{\infty} C_k \left( \frac{g}{a\epsilon(0)} \right)^{k+1} \\ &\quad \times r^k [(k+1) \cos\theta \mathbf{e}_r - \sin\theta \mathbf{e}_\theta] \\ &= A_1 E_0 \sum_{k=0}^{\infty} C_k \left( \frac{g}{a\epsilon(0)} \right)^{k+1} \\ &\quad \times r^k \{ k \cos\theta \sin\theta \cos\phi \mathbf{e}_x + k \cos\theta \sin\theta \sin\phi \mathbf{e}_y \\ &\quad \times [(k+1) \cos^2\theta + \sin^2\theta] \mathbf{e}_z \}. \end{aligned} \quad (20)$$

Then, the corresponding displacement admits

$$\begin{aligned} \mathbf{D}_c &= \bar{\epsilon}_1(r) \cdot \mathbf{E}_c = A_1 E_0 \sum_{k=0}^{\infty} C_k \left( \frac{g}{a\epsilon(0)} \right)^{k+1} \\ &\quad \times r^k [\epsilon_{1r}(r)(k+1) \cos\theta \mathbf{e}_r - \epsilon_{1t}(r) \sin\theta \mathbf{e}_\theta] \\ &= A_1 E_0 \sum_{k=0}^{\infty} C_k \left( \frac{g}{a\epsilon(0)} \right)^{k+1} r^k \{ [\epsilon_{1r}(r)(k+1) \\ &\quad - \epsilon_{1t}(r)] \cos\theta \sin\theta \cos\phi \mathbf{e}_x + [\epsilon_{1r}(r)(k+1) - \epsilon_{1t}(r)] \\ &\quad \times \cos\theta \sin\theta \sin\phi \mathbf{e}_y + [\epsilon_{1r}(r)(k+1) \cos^2\theta \\ &\quad + \epsilon_{1t}(r) \sin^2\theta] \mathbf{e}_z \}. \end{aligned} \quad (21)$$

where  $\mathbf{e}_r$  and  $\mathbf{e}_\theta$  ( $\mathbf{e}_x$ ,  $\mathbf{e}_y$  and  $\mathbf{e}_z$ ) are the unix vectors in spherical coordinates (Cartesian coordinates).

In the dilute limit, from equation (4), we can obtain the effective linear dielectric constant as

$$\begin{aligned} \epsilon_e &= \epsilon_2 + \frac{1}{V E_0} \int_{\Omega_i} (\bar{\epsilon}_1(r) \cdot \mathbf{E} - \epsilon_2 \mathbf{E}) \cdot \mathbf{e}_z dV \\ &= \epsilon_2 + 3f\epsilon_2 \frac{[\epsilon(0) - \epsilon_2] v_1 + g v_3 + 2h v_4}{[\epsilon(0) + g] v_2 + 2\epsilon_2 v_1}, \end{aligned} \quad (22)$$

where

$$\begin{aligned} v_3 &= \sum_{k=0}^{\infty} C_k \frac{1+k}{4+k} \left( \frac{g}{\epsilon(0)} \right)^{k+1} \quad \text{and} \\ v_4 &= \sum_{k=0}^{\infty} C_k \frac{1}{4+k} \left( \frac{g}{\epsilon(0)} \right)^{k+1}. \end{aligned}$$

On the other hand, the substitution of equation (20) into equation (5) yields

$$\begin{aligned} \chi_e &= \frac{1}{V} \sum_{ijkl} \int_{\Omega_i} \chi_{ijkl} E_i E_j E_k E_l^* dV \\ &= f [(\chi_{xyxy} + \chi_{yxxy} + \chi_{xyyx} + \chi_{xyyx} + \chi_{yxyx} + \chi_{yyxx} \\ &\quad + 3\chi_{xxxx} + 3\chi_{yyyy}) U_{q1} (\chi_{xxzz} + \chi_{zzxx} + \chi_{zzxx} \\ &\quad + \chi_{yyzz} + \chi_{zyyz} + \chi_{zyyz}) U_{q2} + (\chi_{zzxx} + \chi_{zzxx} \\ &\quad + \chi_{zzxx} + \chi_{zzyy} + \chi_{yzzz} + \chi_{zyzy}) U_{q3} + \chi_{zzzz} U_{q4}], \end{aligned} \quad (23)$$

where

$$\begin{aligned}
U_{q1} &= \frac{1}{105} |A_2|^2 A_2^2 \sum_{k_1=0}^{\infty} \sum_{k_2=0}^{\infty} \sum_{k_3=0}^{\infty} \sum_{k_4=0}^{\infty} \left\{ \left[ C_{k_1} C_{k_2} C_{k_3} C_{k_4} \right. \right. \\
&\quad \times \left. \left. \left( \frac{g}{\epsilon(0)} \right)^{k_1+k_2+k_3+3} \right] \left[ \left( \frac{g}{\epsilon(0)} \right)^{k_4+1} \right]^* \right. \\
&\quad \times \left. \frac{k_1 k_2 k_3 k_4}{3 + k_1 + k_2 + k_3 + k_4} \right\}, \\
U_{q2} &= 3 |A_2|^2 A_2^2 \sum_{k_1=0}^{\infty} \sum_{k_2=0}^{\infty} \sum_{k_3=0}^{\infty} \sum_{k_4=0}^{\infty} \left\{ \left[ C_{k_1} C_{k_2} C_{k_3} C_{k_4} \right. \right. \\
&\quad \times \left. \left. \left( \frac{g}{\epsilon(0)} \right)^{k_1+k_2+k_3+3} \right] \left[ \left( \frac{g}{\epsilon(0)} \right)^{k_4+1} \right]^* \right. \\
&\quad \times \frac{k_1 k_2}{3 + k_1 + k_2 + k_3 + k_4} \\
&\quad \times \left. \left[ \frac{1}{15} + \frac{1}{35} (k_3 + k_4) + \frac{1}{63} k_3 k_4 \right] \right\}, \\
U_{q3} &= 3 |A_2|^2 A_2^2 \sum_{k_1=0}^{\infty} \sum_{k_2=0}^{\infty} \sum_{k_3=0}^{\infty} \sum_{k_4=0}^{\infty} \left\{ \left[ C_{k_1} C_{k_2} C_{k_3} C_{k_4} \right. \right. \\
&\quad \times \left. \left. \left( \frac{g}{\epsilon(0)} \right)^{k_1+k_2+k_3+3} \right] \left[ \left( \frac{g}{\epsilon(0)} \right)^{k_4+1} \right]^* \right. \\
&\quad \times \frac{k_3 k_4}{3 + k_1 + k_2 + k_3 + k_4} \\
&\quad \times \left. \left[ \frac{1}{15} + \frac{1}{35} (k_1 + k_2) + \frac{1}{63} k_1 k_2 \right] \right\}, \\
U_{q4} &= 3 |A_2|^2 A_2^2 \sum_{k_1=0}^{\infty} \sum_{k_2=0}^{\infty} \sum_{k_3=0}^{\infty} \sum_{k_4=0}^{\infty} \left\{ \left[ C_{k_1} C_{k_2} C_{k_3} C_{k_4} \right. \right. \\
&\quad \times \left. \left. \left( \frac{g}{\epsilon(0)} \right)^{k_1+k_2+k_3+3} \right] \left[ \left( \frac{g}{\epsilon(0)} \right)^{k_4+1} \right]^* \right. \\
&\quad \times \frac{1}{3 + k_1 + k_2 + k_3 + k_4} \\
&\quad \times \left[ 1 + \frac{1}{3} \sum_{i=1}^4 k_i + \frac{1}{5} \sum_{i=1}^3 \sum_{j=i+1}^4 k_i k_j \right. \\
&\quad \times \left. \left. \frac{1}{7} \sum_{i=1}^2 \sum_{j=i+1}^3 \sum_{l=j+1}^4 k_i k_j k_l + \frac{1}{9} k_1 k_2 k_3 k_4 \right] \right\},
\end{aligned}$$

with  $A_2 = (3\epsilon_2) / \{[\epsilon(0) + g]v_2 + 2\epsilon_2 v_1\}$ .

## 5 Numerical results

To illustrate the NADEDA, we first perform numerical calculations for the linear dielectric gradation profiles, that is,  $\epsilon_{1r}(r) = \epsilon(0) + gr/a$  (radial dielectric constant), and  $\epsilon_{1t}(r) = \epsilon(0) + hr/a$  (tangential dielectric constant).

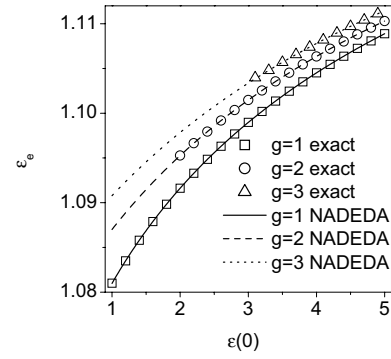


**Fig. 1.** The effective linear dielectric constant ( $\epsilon_e$ ) versus the dielectric constant of the spherical core with radius  $r = 0^+$  [ $\epsilon(0)$ ], for the linear dielectric gradation profiles with various radial gradients  $g$ . Parameters: volume fraction  $f = 0.05$ , the tangential gradient  $h = 8$ . Lines: numerical results obtained from the NADEDA (Eqs. (11) and (17)); Symbols: exact results predicted by the first-principles approach (Eq. (22)). Note that the exact results are available for  $\epsilon(0) > g$ .

In this situation, the exact results for  $\epsilon_e$  and  $\chi_e$  exist, and thus it allows us to show the correctness of the NADEDA. For model calculations, we set  $h > g$  (Note that our formulae can still be used for  $h \leq g$ ). For the NADEDA, we numerically integrate equations (11) and (16) by using *Mathematica* with the initial radius  $r = 0.001$ .

In Figure 1, the effective linear dielectric constant ( $\epsilon_e$ ) is plotted as a function of the dielectric constant of anisotropic graded particles at radius  $r = 0$  [ $\epsilon(0)$ ], for various gradients  $h$  and  $g$ . It is shown that  $\epsilon_e$  increases monotonically with the increase of  $\epsilon(0)$ . Moreover, increasing the gradient  $g$  causes  $\epsilon_e$  to increase as well. This can be understood by the fact that the increases of both  $\epsilon(0)$  and  $g$  lead to the increase of the equivalent dielectric constant  $\bar{\epsilon}(a)$  of the graded particles, thus increasing the effective response of the whole system. For  $\epsilon_e$ , the NADEDA shows good agreement with the first-principles approach.

Next, we investigate the effective third-order nonlinear susceptibility. Let's set the tensorial dielectric susceptibility of the particles to be independent of  $r$ , in an attempt to focus on the nonlinearity enhancement. As a result, it is shown that the nonlinearity enhancement decreases with the increase of  $\epsilon(0)$  and  $g$ . As mentioned above, for larger  $\epsilon_e$  and  $g$ , the graded inclusions possess a larger equivalent dielectric constant, and hence the  $i$ th Cartesian component of the local field should become more weak accordingly. Then, the weaker effective nonlinear susceptibility is obtained. As displayed in Figure 2, we show three typical cases of nonlinearity enhancement. Here, all the physical parameters in use are real, and thus the nonlinearity enhancement for  $\chi_{zzxx}$  (the only nonzero component) is the same as that for  $\chi_{xxzz}$ . Moreover, for other nonzero components of the tensorial nonlinear susceptibility, the nonlinearity enhancement will be the same as one of these shown in Figure 2. For example, Figure 2a can also show the nonlinearity enhancement for  $3\chi_{xxxx}$ ,  $3\chi_{yyyy}$ ,  $\chi_{xyxy}$ , etc. Again, the excellent agreement is numerically

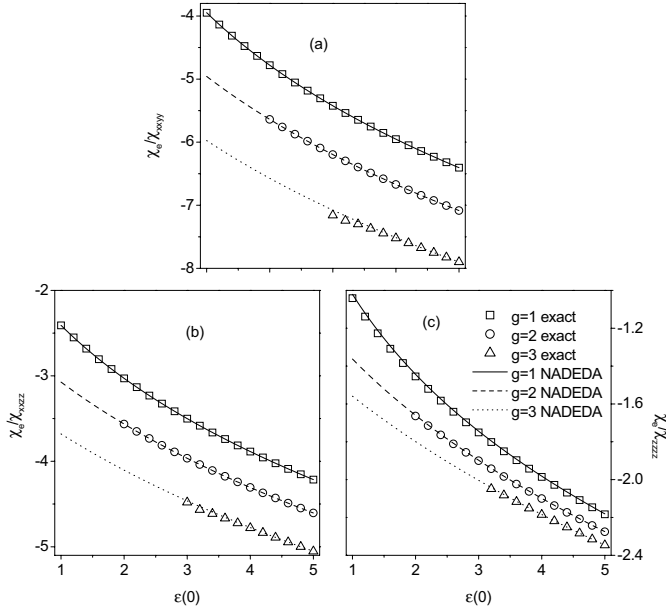


**Fig. 2.** (a)  $\chi_e/\chi_{xyxy}$  versus  $\epsilon(0)$ , for the linear dielectric gradation profiles with various  $g$ , at  $h = 8$ . Here  $\chi_{xyxy}$  is the only nonzero component of the tensorial nonlinear susceptibility. Lines: numerical results obtained from the NADEDA (Eqs. (11), (16) and (18)); Symbols: exact results predicted by the first-principles approach (Eq. (23)). (b) Same as (a), but  $\chi_e/\chi_{xxzz}$  versus  $\epsilon(0)$ , with  $\chi_{xxzz}$  being the only nonzero component. (c) Same as (a), but  $\chi_e/\chi_{zzzz}$  versus  $\epsilon(0)$ , with  $\chi_{zzzz}$  being the only nonzero component.

demonstrated between the first-principles approach and the NADEDA (Eqs. (11, 16) and (18)).

In what follows, we shall investigate the surface plasma resonance effect on the nonlinear metal-dielectric composite. As a model calculation, we assume the radial and tangential dielectric constants for the graded metal particles to be Drude-like, namely,

$$\epsilon_{1r}(r) = 1 - \frac{\omega_{pr}^2(r)}{\omega(\omega + i\gamma)} \quad \text{and} \quad \epsilon_{1t}(r) = 1 - \frac{\omega_{pt}^2(r)}{\omega(\omega + i\gamma)} \quad (24)$$

where  $\omega_{pr}(r)$  and  $\omega_{pt}(r)$  are the radius-dependent radial and tangential plasma frequencies, respectively, and  $\gamma$  is the damping coefficient. For the linear dielectric host, we choose  $\epsilon_2 = 1.77$  (a typical dielectric constant of water). We further assume  $\omega_{pr}(r)$  and  $\omega_{pt}(r)$  to be

$$\omega_{pr}(r) = \omega_p \left(1 - k_r \cdot \frac{r}{a}\right), \quad \text{and} \\ \omega_{pt}(r) = \omega_p \left(1 - k_t \cdot \frac{r}{a}\right), \quad r < a. \quad (25)$$

The above form is quite physical for  $0 < k_r(k_t) < 1$ , since the center of grains can be better metallic so that  $\omega_p(r)$  is larger, while the boundary of the grain may be poorer metallic so that  $\omega_p(r)$  is much smaller. In fact, such a variation can also appear owing to the temperature effect [23]. Moreover, we choose  $k_t \leq k_r$ , in view of the strong metallic behavior in the tangential direction.

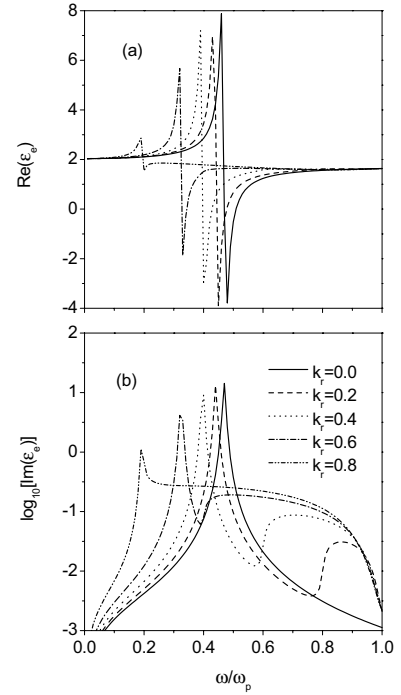


**Fig. 3.** The real and imaginary parts of  $\epsilon_e$  versus frequency  $\omega/\omega_p$ , for various  $k_r$ . Parameters:  $\omega_p/\gamma = 0.01$  and  $k_t = 0$ .

Figure 3 displays the real and imaginary parts of effective dielectric constant  $\epsilon_e$  as a function of the incident angular frequency  $\omega/\omega_p$ . For  $k_r = 0$ , there exists a frequency region, where the real part of the effective dielectric constant is negative. With increasing  $k_r$ , this region becomes narrow generally, in accompanied with less negative  $\text{Re}(\epsilon_e)$  (see Fig. 3a). This is due to the fact that increasing  $k_r$  decreases the influence of the metallic behavior (owing to the decrease of  $\omega_{pr}(r)$ ). In the mean time, the sharp peak for  $\text{Im}(\epsilon_e)$  turn weak with  $k_r$  (see Fig. 3b). Furthermore, for  $k_r \neq 0$ , the continuous resonant bands in the high frequency region appear always, and this region becomes more broad as  $k_r$  increases. In this case, the appearance of the resonant bands results from the radius-dependent plasma frequency  $\omega_p(r)$ . This phenomenon has already been observed, when a shell model [24] or non-spherical model [25] was taken into account. In our previous works [24, 25], a broad continuous spectrum is shown to be around the larger pole in the corresponding spectral density function. Here, the graded particles under consideration can be regarded as a construction of multi shells, which hence should be expected to yield the broader spectra for the optical absorption ( $\text{Im}(\epsilon_e)$ ). In addition, we note that, as  $k_r$  increases, both the surface plasma frequency and the center of resonant bands are red-shifted. In particular, for larger  $k_r$ , the resonant bands can become broader, owing to strong inhomogeneity inside the particles.

Then, we speculate on how gradation and anisotropy affect the optical nonlinearity enhancement in metal-dielectric composites. As shown in Figure 4, no matter

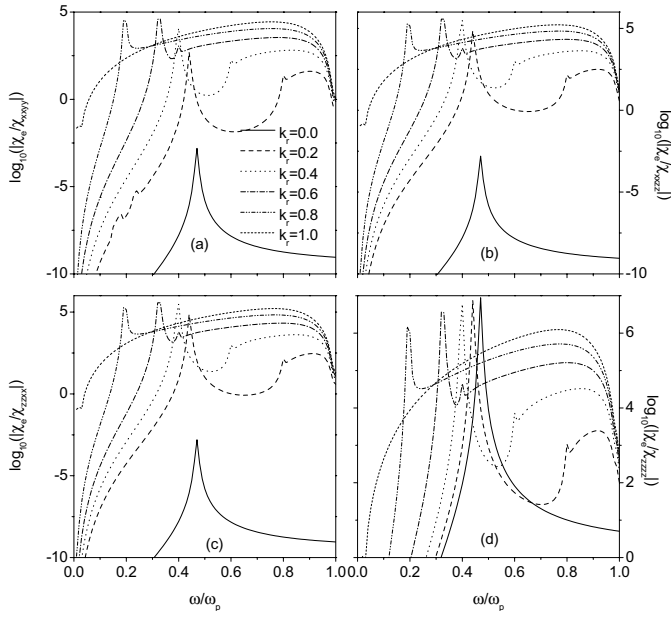


**Fig. 4.** Same as Figure 3, but (a)  $|\chi_e/\chi_{xyy}|$  versus  $\omega/\omega_p$ , with  $\chi_{xyy}$  being the only nonzero component. (b)  $|\chi_e/\chi_{xzz}|$  versus  $\omega/\omega_p$ , with  $\chi_{xzz}$  being the only nonzero component. (c)  $|\chi_e/\chi_{zzxx}|$  versus  $\omega/\omega_p$ , with  $\chi_{zzxx}$  being the only nonzero component. (d)  $|\chi_e/\chi_{zzzz}|$  versus  $\omega/\omega_p$ , with  $\chi_{zzzz}$  being the only nonzero component.

which component of the nonlinear susceptibility tensor is nonzero,  $\chi_e$  can be substantially enhanced within a certain frequency region. In particular, this enhancement becomes quite strong for  $\chi_{zzzz}$  (the only nonzero component). In fact, the physical origin of this huge enhancement is the large increase in the local field component  $E_z$ . In addition, the nonlinearity enhancement will become more strong, for the system with a larger  $k_r$ , which is related to a higher contrast between  $\epsilon_{1t}$  and  $\epsilon_{1r}$ . For example,  $|\chi_e/\chi_{zzzz}| > 10^4$  in the frequency region  $0.2 \leq \omega/\omega_p \leq 1.0$  for  $k_r = 1$ . From Figure 4, we also find that the optical nonlinearity enhancement obtained for four nonzero components, respectively, displays the similar qualitative behaviors. This should be in contrast to those observed in a polycrystalline quasi-one-dimensional conductor [18,20,26], where the effective optical nonlinearity for four elements of the nonlinear susceptibility tensor exhibit quite different behaviors [18] (the differences become more distinct by using spectral representation approximation [20]). Actually, the differences result from two different kinds of dielectric anisotropy (and hence two different kinds of tensorial dielectric constants) under consideration. In this work, we focus on the particles with spatially varying, but spherically symmetric, dielectric anisotropy, whereas, in the previous works [18,20,26], the authors studied uniaxial anisotropy in the Cartesian coordinate system.

Although the optical nonlinearity enhancements for four typical nonzero components of the nonlinear susceptibility ( $\chi_{ijkl}$ ) take on quite similar behaviors, their contributions to the magnitude of the effective optical non-

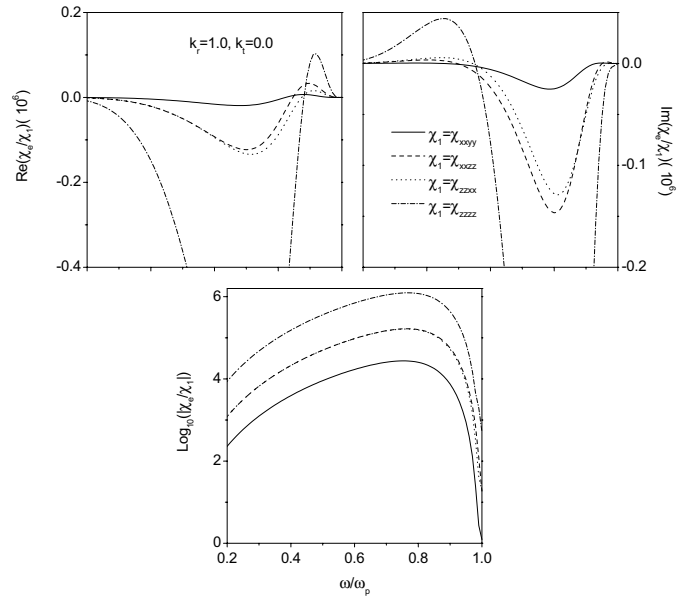


**Fig. 5.** The real and imaginary parts, and the modulus of the optical nonlinearity enhancement for  $k_r = 1$  and  $k_t = 0$ .

linearity are different (see Fig. 5). As shown in Figure 5, the strongest (weakest) nonlinearity enhancement occurs for the case with  $\chi_{zzzz}$  ( $\chi_{xyy}$ ) being only nonzero component. Moreover, the differences between the two cases of  $\chi_{xzz} \neq 0$  only and  $\chi_{zzxx} \neq 0$  only are clearly shown for  $\text{Re}(\chi_e/\chi_1)$  and  $\text{Im}(\chi_e/\chi_1)$ .

For practical applications, a most useful parameter is the figure of merit (FOM), which is defined as the ratio of  $|\chi_e|$  to  $\text{Im}(\epsilon_e)$ . In Figure 6, we investigate the figure of merit. Here the only nonzero component is assumed to be  $\chi_{zzzz}$ . We find that the increase of  $k_r$  (namely, the rapid decrease of the radial metallic behavior) results in a large enhancement of the FOM, especially in the high frequency range (see Fig. 6a). However, the increase of  $k_t$  (i.e., the rapid decrease of the tangential metallic behavior) causes the FOM in the high-frequency region to decrease (see Fig. 6b). For instance, we attain  $\text{FOM} > 10^5$  (which is quite large) in the frequency region  $0.3 \leq \omega/\omega_p \leq 1.0$  for  $k_r = 0.6$  and  $k_t = 0$ . Therefore, it is possible to achieve a large figure of merit by introducing the radial gradation and keeping the tangential dielectric constant unchanged.

## 6 Discussion and conclusion

Here some comments are in order. In this work, we have developed an NADEDA (nonlinear anisotropic differential effective dipole approximation) to investigate the effective linear dielectric constant and third-order nonlinear susceptibility of composite media consisting of nonlinear inclusions with spatially varying dielectric anisotropy. Alternatively, based on the first-principles approach, we have derived the exact expressions for  $\epsilon_e$  and  $\chi_e$ , for the linear dielectric-constant profiles with small slopes. To our interest, excellent agreement is found between the



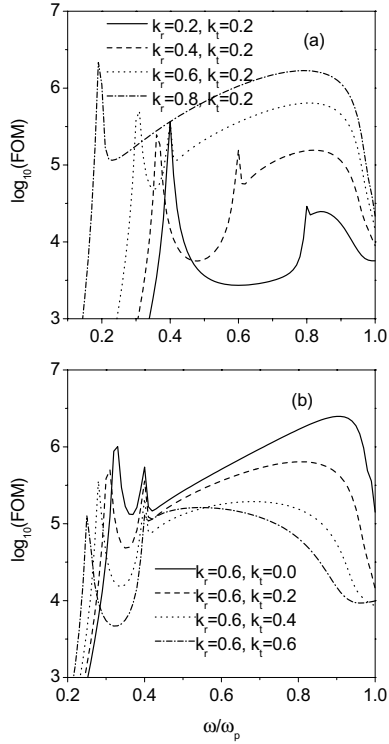


**Fig. 6.** The figure of merit  $\equiv |\chi_e/\chi_{zzzz}|/\text{Im}(\epsilon_e)$  versus  $\omega/\omega_p$ , with  $\chi_{zzzz}$  being the only nonzero component.

approximation results (NADEDA) and the exact results (first-principles approach). It is worth noting that exact solutions are very few in composite research, and thus our NADEDA provides an effective way to estimate the effective nonlinear properties in composite media consisting of anisotropic graded inclusions.

An application, we apply the NADEDA to study the surface plasma resonance effect on the effective linear dielectric constant, the optical nonlinearity enhancement and the figure of merit in metal-dielectric composites, in which the metal particles possess the tensorial dielectric constants with dielectric gradation profiles. It is found that the gradation profiles in radial dielectric constants are a useful way to control the local-field effects, thus being able to enhance the figure of merit hugely.

The present methods are strictly valid in the dilute limit. The presence of both gradation and dielectric anisotropy is shown to be helpful to achieve the large figure of merit, but unable to realize the separation of the absorption peak from the nonlinearity enhancement peak. In this regard, we may intentionally manipulate composite microstructures, e.g., by using the shape distribution of graded inclusions [27], and by using fractal [28] and anisotropic microstructures [29] with large volume fractions. When the volume fraction of graded inclusions is large, percolation behaviors can occur. To this end, the further broadening of the enhancement peak as well as the desired separation of the optical absorption from the nonlinearity peak is expected to be realized.

Our work can be generalized to the nonlinear composites of anisotropic graded inclusions, which is subject to an external alternating current (AC) electric field. For a sinusoidal applied field, the electric response in the composites will generally consist of AC fields at frequencies of high-order harmonics. Initial results show that the fundamental and third-order harmonic AC responses are sensitive to the dielectric gradation profiles as well as anisotropy. Thus, by measuring the AC responses of the anisotropic graded composites, it is possible to perform a real-time monitoring of the fabrication process of the gradation profiles within the particles.

To sum up, we put forth an NADEDA (nonlinear anisotropic differential effective dipole approximation) in this work, in an attempt to discuss the effects of gradation as well as anisotropy on the optical properties of composite media. For the linear dielectric-constant profiles, the NADEDA has been numerically demonstrated in good agreement with the first-principles approach. To our great interest, both the huge nonlinearity enhancement and the large figure of merit are shown to be achievable by the presence of gradation as well as local anisotropy inside the inclusions.

This work has been supported by the Research Grants Council of the Hong Kong SAR Government under project numbers CUHK 4245/01P and CUHK 403303, by the National Natural Science Foundation of China under Grant No. 10204017 (L.G.), and by the Natural Science of Jiangsu Province under Grant No. BK2002038 (L.G.). We thank Prof. G.Q. Gu for his fruitful discussion.

## References

1. M. Yamanouchi, M. Koizumi, T. Hirai, I. Shioda, in *Proceedings of the First International Symposium on Functionally Graded Materials* (Sendi, Japan, 1990)
2. Z.H. Jin, N. Noda, *Int. J. Eng. Sci.* **31**, 793 (1993)
3. A.J. Sanchez-Herencia, R. Mereno, J.R. Jurado, *J. Eur. Ceram. Soc.* **20**, 1611 (2000)
4. E. Erdogan, A.C. Kaya, P.E. Joseph, *J. Appl. Mech.* **58**, 410 (1991)
5. S. Chandrasekhar, *Liquid Crystals*, 2nd edn. (Cambridge University Press, Cambridge, 1992)
6. A.M. Freyria, E. Chignier, J. Guidollet, P. Louisot, *Biomaterials* **12**, 111 (1991)
7. L. Dong, G.Q. Gu, K.W. Yu, *Phys. Rev. B* **67**, 224205 (2003)
8. G.Q. Gu, K.W. Yu, *J. Appl. Phys.* **94**, 3376 (2003)
9. J. P. Huang, K.W. Yu, G.Q. Gu, M. Karttunen, *Phys. Rev. E* **67**, 051405 (2003)
10. K.W. Yu, G.Q. Gu, J.P. Huang, *cond-mat/0211532* (unpublished)
11. M. Avellaneda, A.V. Cherkov, K.A. Lurie, G.W. Milton, *J. Appl. Phys.* **63**, 4989 (1988), and references therein
12. J.H. Erdmann, S. Zumer, J.W. Doane, *Phys. Rev. Lett.* **64**, 1907 (1990)
13. V.L. Sukhorukov, G. Meedt, M. Kürschner, U. Zimmermann, *J. Electrostat.* **50**, 191 (2001)

14. D.J. Bergman, D. Stroud, *Solid State Physics: Advances in Research and Applications*, edited by H. Ehrenreich, D. Turnbull (Academic Press, New York, 1992), Vol. 46, p. 147
15. See, for example, the articles in *Proceedings of the 5th International Conference on Electrical Transport and Optical Properties of Inhomogeneous Media*, edited by P.M. Hui, Ping Sheng, L.H. Tang, Physica B **279** (2000)
16. A.K. Sarychev, V.M. Shalaev, Phys. Rep. **335**, 275 (2000), and references cited therein
17. H. Karacali, S.M. Risser, K.F. Ferris, Phys. Rev. E **56**, 4286 (1997)
18. D. Stroud, Phys. Rev. B **54**, 3295 (1996)
19. D. Stroud, P.M. Hui, Phys. Rev. B **37**, 8719 (1988)
20. S. Barabash, D. Stroud, J. Phys.: Condens. Matter **11**, 10323 (1999)
21. K.W. Yu, P.M. Hui, D. Stroud, Phys. Rev. B **47**, 14150 (1993)
22. G.W. Milton, *The Theory of Composites*, Chap. 7 (Cambridge University Press, Cambridge, 2002)
23. L. Gao, Z.Y. Li, J. Appl. Phys. **91**, 2045 (2002)
24. L. Gao, J.T.K. Wan, K.W. Yu, Z.Y. Li, J. Appl. Phys. **88**, 1893 (2000)
25. L. Gao, J.T.K. Wan, K.W. Yu, Z.Y. Li, J. Phys.: Condens. Matter **12**, 6825 (2000)
26. O. Levy, D. Stroud, Phys. Rev. B **56**, 8035 (1997)
27. L. Gao, K.W. Yu, Z.Y. Li, B. Hu, Phys. Rev. E **64**, 036615 (2001)
28. V.M. Shalaev, *Nonlinear Optics of Random Media: Fractal Composites and Metal-Dielectric Films* (Springer-Verlag, Berlin, 2000), and references therein
29. K.P. Yuen, M.F. Law, K.W. Yu, Ping Sheng, Phys. Rev. E **56**, R1322 (1997)